Article

Dissociation Reactions of Free Tetrapyridinium Tetracations and of Their Catenanes

Jana Roithov, Petr Milko, Claire L. Ricketts, Detlef Schrder, Thierry Besson, Vclav Dekoj, and Martin Blohradsk

J. Am. Chem. Soc., **2007**, 129 (33), 10141-10148• DOI: 10.1021/ja071058h • Publication Date (Web): 26 July 2007

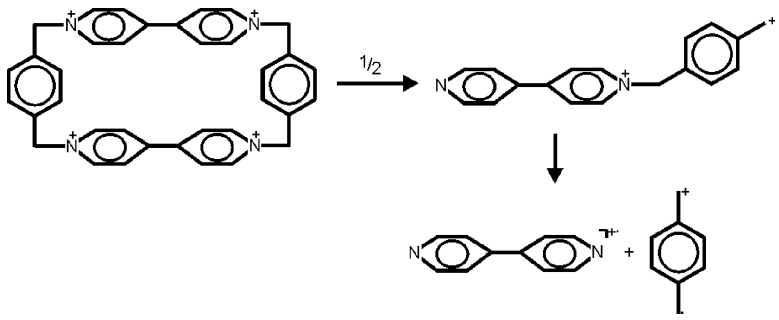

More About This Article

Additional resources and features associated with this article are available within the HTML version:

- Supporting Information
- Links to the 7 articles that cite this article, as of the time of this article download
- Access to high resolution figures
- Links to articles and content related to this article
- Copyright permission to reproduce figures and/or text from this article

View the Full Text HTML

J|A|C|S
ARTICLES
Published on Web 07/26/2007

Dissociation Reactions of Free Tetrapyridinium Tetracations and of Their Catenanes

Jana Roithová,[#,‡] Petr Milko,[#] Claire L. Ricketts,[#] Detlef Schröder,*[,#] Thierry Besson,[§] Václav Dekoj,[#] and Martin Bělohradský[#]

Contribution from the Institute of Organic Chemistry and Biochemistry, Flemingovo nám. 2, 16610 Prague 6, Czech Republic, Department of Organic Chemistry, Charles University, Hlavova 8, 12843 Prague 2, Czech Republic, and Laboratoire Chimie-Physique, UMR8000, Université Paris-Sud, 91405 Orsay Cedex, France

Received February 14, 2007; E-mail: detlef.schroeder@uochb.cas.cz

Abstract: Electrospray ionization from methanolic solution can be used for the generation of the free cyclophane tetracations $\mathbf{1}^{4+}$–$\mathbf{3}^{4+}$ from the corresponding hexafluorophosphates. In the idealized gas phase, these tetracations are long-lived and can easily be handled for further spectroscopic studies. Collision-induced dissociation of the free tetracations brings about charge separation via cleavage of the pyridinium bonds, leading to a pair of dications. Subsequently, these dications undergo another charge separation reaction to finally afford singly charged cations. In addition to the free tetracations, also the corresponding trications having one PF_6^- counterion are examined. Collision-induced dissociation of the trications leads to a formal substitution reaction concomitant with C–F bond formation. Further, the catenanes of the tetracations $\mathbf{1}^{4+}$–$\mathbf{3}^{4+}$ with bis-*p*-phenylene-34-crown-10 (**4**) are investigated. For the parent compound **1**, also the gas-phase infrared spectrum is reported for the first time.

1. Introduction

In 1988, Stoddart and co-workers described the synthesis of the tetracationic cyclobis(paraquat-*p*-phenylene) $\mathbf{1}^{4+}$ with several counterions; for $[\mathbf{1}^{4+}\cdot 4PF_6^-]$ with additional acetonitrile molecules in the crystal, an X-ray structure was reported.[1,2] The four pyridinium ions induce a high charge density in the inner volume of the macrocycle, which can hence serve as a host for electron-rich arenes, such as dialkoxybenzenes.

In the course of continuous studies of multiply charged ions,[3−5] we became interested in this topic from a fundamental point of view. Our key question in this respect is whether $\mathbf{1}^{4+}$ can withstand the Coulomb forces exerted by the 4-fold positive charge also in the absence of any stabilizing counterions or solvent molecules,[6,7] that is, whether the free tetracation $\mathbf{1}^{4+}$ does also exist in the gas phase.[8] In addition to the parent compound $[\mathbf{1}^{4+}\cdot 4PF_6^-]$, also the homologues $[\mathbf{2}^{4+}\cdot 4PF_6^-]$ and $[\mathbf{3}^{4+}\cdot 4PF_6^-]$ as well as their catenanes with bis-*p*-phenylene-34-crown-10 (**4**) are studied, for example, **cat-1**$^{4+}$ (Chart 1).[9]

2. Experimental Section

The experiments were performed with a TSQ Classic mass spectrometer of QOQ configuration (Q stands for quadrupole and O for octopole) which has been described elsewhere.[10] In the present experiments, electrospray ionization was used for ion generation. The ions of interest were then mass-selected by means of Q1 at mass resolutions sufficient to fully resolve the natural ^{13}C-contributions of the molecular cations (see below). Collision-induced dissociation (CID) at elevated kinetic energies was performed in the octopole using xenon as a collision gas, and the product ions formed were subsequently mass-analyzed using Q2, for which again a mass resolution fully sufficient to analyze multiply charged species was adjusted. In several cases, the multiply charged ions containing one ^{13}C atom were selected to avoid isobaric interferences.[11] In the case of the catenanes **cat-2**$^{4+}$ and **cat-3**$^{4+}$, however, the absolute ion currents were very low, and the mass resolution in ion selection was hence reduced to a unit mass (see below). For the high-resolution mass determination of $\mathbf{1}^{4+}$ and $[\mathbf{1}^{4+}\cdot PF_6^-]$, an ApexQe hybrid Qh FT-ICR mass spectrometer with an Apollo II ESI source was used.

Gas-phase infrared spectra were recorded with a Bruker Esquire 3000 ion-trap mass spectrometer (IT–MS)[12] mounted to the beam line of a

[#] Institute of Organic Chemistry and Biochemistry.
[‡] Charles University.
[§] Université Paris-Sud.

(1) Odell, B.; Reddington, M. V.; Slawin, A. M. Z.; Spencer, N.; Stoddart, J. F.; Williams, D. J. *Angew. Chem., Int. Ed. Engl.* **1988**, *27*, 1547.
(2) See also: (a) Asakawa, M.; Dehaen, W.; L'abbe, G.; Menzer, S.; Nouwen, J.; Raymo, F. M.; Stoddart, J. F.; Williams, D. J. *J. Org. Chem.* **1996**, *91*, 9591. (b) Asakawa, M.; Ashton, P. R.; Menzer, S.; Raymo, F. M.; Shimizu, G. K. H.; Stoddart, J. F.; Williams, D. J. *Chem.–Eur. J.* **1996**, *2*, 877.
(3) (a) Schröder, D.; Schwarz, H. *J. Phys. Chem. A* **1999**, *103*, 7385. (b) Schröder, D.; Schwarz, H. *J. Phys. Chem. A* **1999**, *103*, 7385.
(4) Schröder, D. *Angew. Chem., Int. Ed.* **2004**, *43*, 1329.
(5) Roithová, J.; Schröder, D. *Phys. Chem. Chem. Phys.* **2007**, *9*, 2341.
(6) For theoretical even more extreme cases of molecular tetracations, see: (a) Wong, M. W.; Nobes, R. H.; Radom, L. *J. Chem. Soc., Chem. Commun.* **1987**, 233. (b) Olah, G. A.; Rasul, G. *J. Am. Chem. Soc.* **1996**, *118*, 12922. (c) Harvey, J. N.; Kaczorowska, M. *Int. J. Mass Spectrom.* **2003**, *228*, 517.
(7) For a previous prediction of microsolvated tetracations, also see: Shvartsburg, A. A. *J. Am. Chem. Soc.* **2002**, *124*, 12343.
(8) The extended aromatic backbone of the tetrapyridinium skeleton allows an extensive delocalization of the charge, thereby stabilizing the tetracations, see also: (a) Dixon, D. A.; Calabrese, J. C.; Harlow, R. L.; Miller, J. S. *Angew. Chem., Int. Ed. Engl.* **1989**, *28*, 92. (b) Bock, H.; Nick, S.; Bats, J. W. *Tetrahedron Lett.* **1992**, *33*, 5941.
(9) For earlier studies of catenanes using electrospray ionization, see: Amabilino, D. B.; et al. *J. Am. Chem. Soc.* **1995**, *117*, 1271 and references cited therein.
(10) Roithová, J.; Schröder, D. *Phys. Chem. Chem. Phys.* **2007**, *9*, 731.
(11) Roithová, J.; Schröder, D.; Schwarz, H. *Chem.–Eur. J.* **2005**, *11*, 628.
(12) Mac Aleese, L.; Simon, A.; McMahon. T. B.; Ortega, J. M.; Scuderi, D.; Lemaire, J.; Maitre, P. *Int. J. Mass Spectrom.* **2006**, *249*, 14.

Chart 1. Structures of the Tetracations $\mathbf{1}^{4+}$−$\mathbf{3}^{4+}$ Investigated in This Work[a]

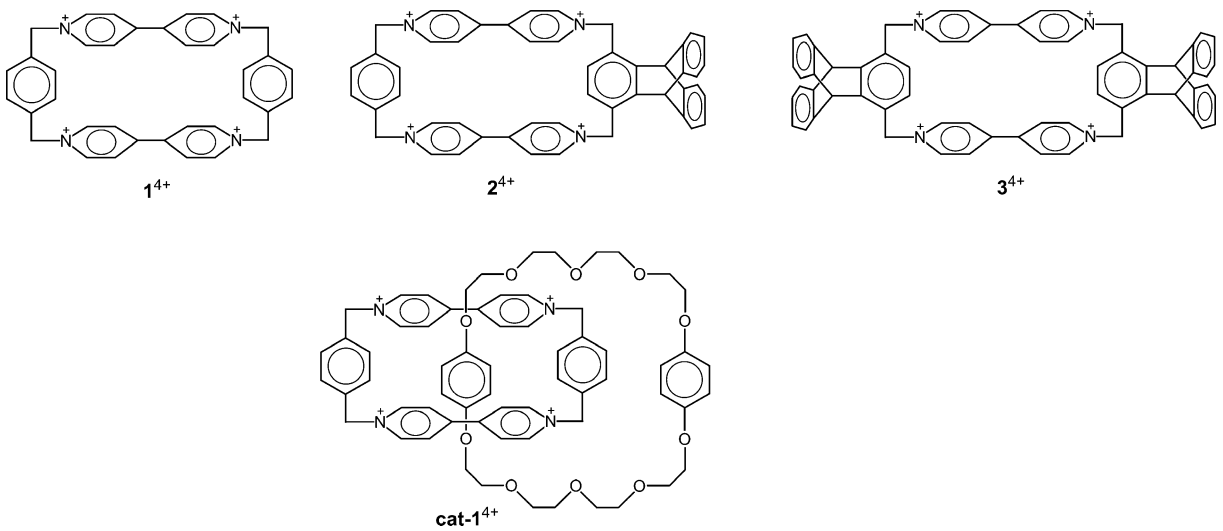

[a] In addition, the corresponding trications bearing one PF_6^- counterion and the catenanes with the macrocyclic polyether **4** are examined; only the catenane **cat-1**$^{4+}$ consisting of the cation $\mathbf{1}^{4+}$ and the ether **4** is shown here.

free electron laser at CLIO (Centre Laser Infrarouge Orsay, France). Briefly, the ions of interest, $\mathbf{1}^{4+}$, [$\mathbf{1}^{4+}$·PF_6^-], and **cat-1**$^{4+}$ were generated by ESI of methanolic solutions of [$\mathbf{1}^{4+}$·$4PF_6^-$] and [**cat-1**$^{4+}$·$4PF_6^-$], respectively, and mass-selected in the ion trap. While the mass resolution of the IT−MS was not sufficient to fully resolve the ^{13}C-isotope pattern of the tetracations, the overall ESI mass spectra closely resembled those obtained with the TSQ Classic under conditions, where no dications are formed. Moreover, closer inspection of the peak profiles in the IT−MS measurements reveals changes in slope on the high-mass shoulder of the signals assigned to the tetracations. Further, at deliberately enforced ionization conditions, the isotope pattern of the dicationic fragments of $\mathbf{6}^{2+}$ could clearly be resolved in IT−MS. Hence, we conclude safely that the genuine tetracations have been sampled in the IRMPD studies. Note, however, that because of the limited mass resolution, the primary fragmentation of the tetracation cannot be monitored in the IT−MS, and the monocationic fragments resulting from consecutive fragmentation were considered instead (see later). After mass selection, infrared multiphoton dissociation was induced by admittance of 1−4 pulses of IR-laser light to the ion trap. In the 40−45 MeV range in which CLIO was operated in these experiments, the IR light covers a range from about 900−1800 cm^{-1}. Effects of laser-power dependence and irradiation time were checked for in appropriate control experiments, and no other than the expected dependences were found.[13,14]

Complementary calculations of the parent tetracation $\mathbf{1}^{4+}$, its fragment $\mathbf{6}^{4+}$, and the hexafluorophosphate adduct [$\mathbf{1}^{4+}$·PF_6^-] were performed using the density functional theory method B3LYP[15−17] in conjunction with 6-31G** triple-ζ basis set as implemented in the Gaussian 03 suite.[18] The reported structures represent the global minima found in this study. The search for different conformers led in the case of tetracation $\mathbf{1}^{4+}$ to two structures with slightly different mutual orientation of the bipyridyl rings and lying within 0.1 eV in energy. The IR spectra of these conformers are indistinguishable. As to the hexafluorophosphate adduct [$\mathbf{1}^{4+}$·PF_6^-], the inclusion of PF_6^- to both conformers of $\mathbf{1}^{4+}$ leads to the same minimum. Attempts to find a complex with PF_6^- on the outer side of $\mathbf{1}^{4+}$ always led to the inclusion of the anion into the macrocycle during the optimization procedure. For all optimized structures, frequency analysis at the same level of theory was performed to assign them as genuine minima or transition structures on the potential-energy surface as well as to calculate the IR frequencies. The computed frequencies were scaled with a factor of 0.9614 as recommended by Scott and Radom.[19,20] For better comparison with the experimental spectra, the computed data were Gaussian-broadened with a half width of 30 cm^{-1}, which corresponds to the range of the experimental resolution of the IRMPD spectra at CLIO.

Compounds [$\mathbf{1}^{4+}$·$4PF_6^-$], [$\mathbf{2}^{4+}$·$4PF_6^-$], [$\mathbf{3}^{4+}$·$4PF_6^-$], and their catenanes were made according to standard procedures following the work of Stoddart et al.,[1] and further details are given in the Supporting Information.

3. Results and Discussion

Here, we describe the gas-phase fragmentation of the free tetracations $\mathbf{1}^{4+}$−$\mathbf{3}^{4+}$, the corresponding trications with one hexafluorophosphate as a counterion, [$\mathbf{1}^{4+}$·PF_6^-]−[$\mathbf{3}^{4+}$·PF_6^-], and of their catenanes **cat-1**$^{4+}$−**cat-3**$^{4+}$ with bis-*p*-phenylene-34-crown-10 (**4**). As relatively small gaseous quadruply charged molecular cations have scarcely been described in the literature,[21−23] the results for the parent tetracation $\mathbf{1}^{4+}$ are discussed in some more detail including its gas-phase infrared spectrum and complementary calculations, whereas the experimental results for the other compounds are presented in a more condensed manner.

(13) Le Caer, S.; Ph.D. Thesis, Universite Paris-Sud, Orsay, France, 2003.
(14) Schröder, D.; Schwarz, H.; Milko, P.; Roithová, J. *J. Phys. Chem. A* **2006**, *110*, 8346.
(15) Vosko, S. H.; Wilk, L.; Nusair, M. *Can. J. Phys.* **1980**, *58*, 1200.
(16) Lee, C.; Yang, W.; Parr, R. G. *Phys. Rev. B* **1988**, *37*, 785.
(17) Miehlich, B.; Savin, A.; Stoll, H.; Preuss, H. *Chem. Phys. Lett.* **1989**, *157*, 200.
(18) *Gaussian 03*; Revision C.02, Gaussian, Inc.: Wallingford, CT, 2004.
(19) Scott, A. P.; Radom, L. *J. Phys. Chem.* **1996**, *100*, 16502.
(20) See also: Andersson, M. P.; Udval, P. *J. Phys. Chem. A* **2005**, *109*, 2937.
(21) For selected examples of free organic tetracations, see: (a) Bursey, M. M.; Rogerson, P. F.; Bursey, J. M. *Org. Mass Spectrom.* **1970**, *4*, 615. (b) Chan, K. W. S.; Cook, K. D. *Org. Mass Spectrom.* **1983**, *18*, 423. (c) Tang, X. J.; Thibault, P.; Boyd, R. K. *Anal. Chem.* **1993**, *65*, 2824. (d) Takayama, M. *Int. J. Mass Spectrom.* **1996**, *152*, 1. (e) Senn, G.; Märk, T. D.; Scheier, P. *J. Chem. Phys.* **1998**, *108*, 990.
(22) For selected examples of metal-containing gaseous tetracations, see: (a) Arakawa, R.: Matsubayashi, G.; Ohashi, N.; Furuuchi, S.; Matsuo, T.; Ali, M. M.: Haga. M. *J. Mass Spectrom.* **1996**, *31*, 861. (b) Hao, C. Y.; March, R. E.; Croley, T. R.; Smith, J. C.; Rafferty, S. P. *J. Mass Spectrom.* **2001**, *36*, 79. (c) Tomazela, D. M.; Gozzo, F. C.; Mayer, I.; Engelmann, R. M.; Araki, K.; Toma, H. E.; Eberlin, M. N. *J. Mass Spectrom.* **2004**, *39*, 1161. (d) Kraus, T.; Buděšinský, T.; Cvačka, J.; Sauvage, J.-P. *Angew. Chem., Int. Ed.* **2006**, *45*, 258.
(23) For free tetraanions, see: Wang, L. S.; Wang, X. B. *J. Phys. Chem. A* **2000**, *104*, 1978 and references therein.

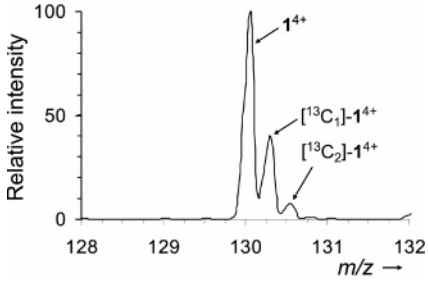

Figure 1. Region of the tetracation $\mathbf{1}^{4+}$ in the ESI mass-spectrum of a dilute methanolic solution of $[\mathbf{1}^{4+}\cdot 4PF_6^-]$. Note the clear separation of the isotope envelope and the signal spacings by 0.25 amu.

Electrospray ionization of a dilute methanolic solution of $[\mathbf{1}^{4+}\cdot 4PF_6^-]$ gives a decent signal corresponding to $\mathbf{1}^{4+}$, $C_{36}H_{32}N_4^{4+}$ with $m/z = 130$ (Figure 1), whose identity as a genuine tetracation is clearly demonstrated by the spacing by 0.25 mass units in conjunction with the isotope pattern (measured, 130.00:130.25:130.50:130.75 ≅ 100:40.2:7.5:0.9; expected,[24] 100:40.7:8.2:1.0).[25] Further, high-resolution mass measurements using Fourier-transform ion cyclotron resonance fully confirm the assignment of the signal at 130 as a genuine tetracation ($m_{exp} = 130.06505$ versus $m_{th} = 130.06513$). Thereby, the experimental data, that is, the mass differences of the isotopic peaks, the isotope pattern, the high-resolution data, and also the fragmentation pattern of the $[^{13}C_1]$-ion described in the next paragraph, provide unambiguous evidence that the free tetracation $\mathbf{1}^{4+}$ can exist as a long-lived species in the idealized gas phase, despite the large intramolecular repulsion resulting from the presence of four Coulomb charges in a relatively small volume. With regard to the lifetime of the tetracation, we note further that the signal due to $\mathbf{1}^{4+}$ was observed for several seconds in the ion-trap apparatus used for the IRMPD experiments, when no infrared radiation was admitted to the trap.

Upon collisional activation, a symmetrical cleavage takes place which leads to two dications according to reaction (1).

$$C_{36}H_{32}N_4^{4+}\ (\mathbf{1}^{4+}) \rightarrow 2C_{18}H_{16}N_2^{2+} \qquad (1)$$

$$[^{13}C_1]\text{-}C_{36}H_{32}N_4^{4+} \rightarrow C_{18}H_{16}N_2^{2+} + [^{13}C_1]\text{-}C_{18}H_{16}N_2^{2+} \qquad (1a)$$

$$C_{18}H_{16}N_2^{2+} \rightarrow C_8H_8^{+} + C_{10}H_8N_2^{+} \qquad (2)$$

Because size and charge of the fragment are exactly half of that of the parent tetracation, this fragmentation cannot be recognized for the *all*-^{12}C compound as parent and fragment ions have the same mass-to-charge ratio. However, mass-selection of the natural $[^{13}C_1]$-isotope (Figure 2a) and subsequent fragmentation reveals the occurrence of reaction 1a, in that the tetracation with $m/z = 130.25$ yields a ca. 1:1 ratio of two dicationic fragments with $m/z = 130.00$ and $m/z = 130.50$, respectively (Figure 2b). Note that despite the limited mass resolution of the multiple setup used, such a fragmentation pattern can only be obtained for a tetracation, in that dissociation of a hypothetical dication with $m/z = 130$ would lead to a mass difference of $\Delta m = 1$ of the fragments, and tri- or pentacations cannot yield this kind of symmetrical cleavage.

On the basis of the mere ion masses, it cannot be decided whether the cleavage involves the central C−C bonds between the two bipyridyl units or the C−N bonds of the pyridinium centers. This lacking information can be gained from consideration of the subsequent dissociation of the dication in which monocations with $m/z = 104$ and $m/z = 156$ are formed (Figure 3) which can be accounted for by a *p*-benzoquinodimethane ion and ionized bipyridyl, respectively (reaction 2). Under the conditions of the CID experiment, ionized bipyridyl also undergoes consecutive dissociations to inter alia afford the fragments $C_{10}H_7N_2^+$ ($m/z = 155$) and $C_5H_4N^+$ ($m/z = 78$).[26]

The consecutive fragmentation of tetracationic $\mathbf{1}^{4+}$ can hence be summarized in terms of Scheme 1, which may serve as guidance for the understanding of the other spectra discussed further below. Hence, we propose that the charge separation of the tetracation is initiated by cleavage of one of the C−N bonds ($\mathbf{1}^{4+} \rightarrow \mathbf{5}^{4+}$), followed by charge-driven stretching of the now acyclic backbone and subsequent cleavage of a second, remote C−N bond, which results in a symmetrical cleavage of the tetracation into two dications ($\mathbf{5}^{4+} \rightarrow 2\mathbf{6}^{2+}$). These dications subsequently undergo another C−N bond cleavage to finally afford the monocations $C_8H_8^+$ and $C_{10}H_8N_2^+$. Whereas the latter most probably corresponds to ionized 4,4′-bipyridyl,[27] a manifold of structures is conceivable for the $C_8H_8^+$ fragment,[28,29] and the *p*-benzoquinodimethane ion shown here is just chosen in resemblance to the structure of the precursor compound.

For the corresponding trication containing one PF_6^- counterion, i.e., $[\mathbf{1}^{4+}\cdot PF_6^-]$ (high resolution: $m_{exp} = 221.74161$ versus $m_{th} = 221.74174$), the major dissociation channel upon CID leads to the formation of $C_{28}H_{24}N_4^{2+}$ dication ($\mathbf{7}^{2+}$) concomitant with a $C_8H_8F^+$ monocation and (presumably) neutral PF_5 (Figure 4).

$$[\mathbf{1}^{4+}\cdot PF_6^-] \rightarrow C_{28}H_{24}N_4^{2+} + C_8H_8F^+ + PF_5 \qquad (3)$$

Reaction 3 can be classified as an intramolecular S_N reaction in which a fluoride ion liberated from the PF_6^- counterion attacks a benzylic position,[30,31] thereby resulting in a first C−N bond cleavage, followed by rupture of the second C−N bond at the same benzoquinodimethane linker.

We note in passing that Figure 4 also points to an instrumental aspect which is associated with the detection of charge-separation products of multiply charged ions in a multipole configuration and is particularly pronounced at high mass resolution. According to the stoichiometric balance, the monocation $C_8H_8F^+$ and the dication $C_{28}H_{24}N_4^{2+}$ are formed in a

(24) Calculated using the Chemputer made by M. Winter, University of Sheffield, see: http://winter.group.shef.ac.uk/chemputer/.
(25) Also see: Tabb, D. L.; Shah, M. B.; Strader, M. B.; Conelly, H. M.; Hettich, R. L.; Hurst, G. B. *J. Am. Soc. Mass Spectrom.* **2006**, *17*, 903.
(26) For the mass spectrum of 4,4′-bipyridyl, see: Stein, S. E. *NIST Standard Reference Database Number 69*; Linstrom, P. J., Mallard W. G., Eds.; NIST Mass Spectrometry Data Center; National Institute of Standards and Technology: Gaithersburg, MD, 2005 (http://webbook.nist.gov).
(27) Maier, J. P.; Turner, D. W. *Faraday Disc. Chem. Soc.* **1972**, *54*, 149.
(28) See: (a) Kuck, D.; Bruder, A.; Ramana, D. V. *Int. J. Mass Spectrom.* **1997**, *167/168*, 55. (b) Freeman, P. K.; Pugh, J. K. *J. Am. Chem. Soc.* **1999**, *121*, 2269. (c) Bally, T.; Bernhard, S.; Matzinger, S.; Truttmann, L.; Zhu, Z. D.; Roulin, J. L.; Marcinek, A.; Gebicki, J.; Williams, F.; Chen, G. F.; Roth, H. D.; Herbertz T. *Chem.—Eur. J.* **2000**, *6*, 849 and references cited therein.
(29) For a review, see: Kuck, D.; Mormann, M. In *The Chemistry of Dienes and Polyenes*; Rappoport, Z., Ed.; Wiley: London, 2000; Vol. 2, p 1.
(30) For this mechanism, see: Gross, D. S.; Williams, E. R. *Int. J. Mass Spectrom.* **1996**, *158*, 305.
(31) See also: Gronert, S.; Fagin, A. E.; Okamoto, K.; Pratt, L. M. *J. Am. Chem. Soc.* **2004**, *126*, 12977 and references therein.

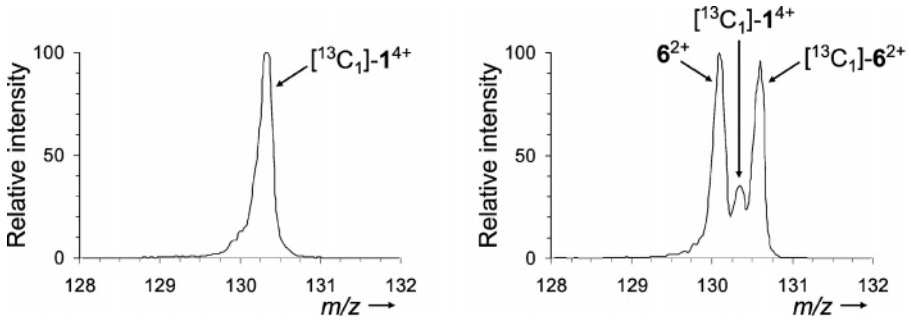

Figure 2. (a) Mass-selected [$^{13}C_1$]-isotope of $\mathbf{1}^{4+}$ in the absence of collision gas; the low-energy tailing of the peak is caused by the collision-energy offset of 25 eV. (b) Parent region of the CID mass-spectrum of [$^{13}C_1$]-$\mathbf{1}^{4+}$ in the presence of xenon as a collision gas (collision energy 25 eV in the laboratory frame). The parent tetracation (center) dissociates into two monocations (left and right) with a spacing of 0.5 amu.

Scheme 1. Sketch of the Consecutive Fragmentation of the Tetracation $\mathbf{1}^{4+}$ via the Dication $\mathbf{6}^{2+}$ (Two Equivalents) to the Monocations $C_8H_8^+$ ($m/z = 104$) and $C_{10}H_8N_2^+$ ($m/z = 156$)

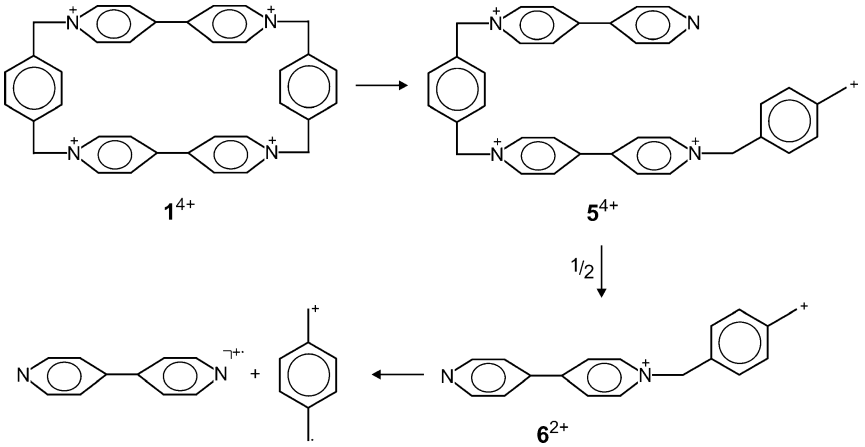

1:1 ratio. Nevertheless, a large preference of the dication is observed in the experiment (Figure 4), which is attributed to a better collection efficiency of the doubly charged fragment in ion detection in conjunction with its larger mass. In comparison, the lighter, singly charged fragment is much more affected by the kinetic energy released upon charge separation of the multiply charged ion.[32]

To the best of our knowledge $\mathbf{1}^{4+}$ is among the smallest tetracations studied so far[21,22] and, moreover, a purely organic one with several C−C− and C−N− single bonds.[33] Given that the structures of multiply charged ions often substantially differ from those of their neutral and also their monocationic counterparts,[34] the identity of the gaseous tetracation was probed further by means of its infrared spectrum.[35] To this end, infrared multiphoton dissociation (IRMPD) of mass-selected ions was applied using the infrared laser CLIO. Because the primary dissociation of $\mathbf{1}^{4+}$ leads to an isobaric dication (see earlier) in conjunction with the fact that the ion-trap mass spectrometer used for the IRMPD experiments could not fully resolve the isotope pattern of the tetracation (see experimental details), the monocationic fragments with $m/z = 104$, 155, and 156 were used as monitors for ion fragmentation. Figure 5 shows the experimental IR spectrum of mass-selected $\mathbf{1}^{4+}$ between 900 and 1800 cm^{-1}, which was spectral range probed at CLIO, along with the computed IR spectra of $\mathbf{1}^{4+}$ (blue) and the dicationic fragment $\mathbf{6}^{4+}$ (red) in this spectral window.

The experimental spectrum (black triangles in Figure 5) is dominated by an intense band at about 1630 cm^{-1} with a half-width of ca. 25 cm^{-1}. According to the calculations, this composite band mainly corresponds to the C−C stretches of the aromatic rings (of both the bipyridyl unit and the xylene spacers). At lower wavenumbers down to about 1100 cm^{-1}, a number of additional adsorptions are identified by experiment with three clear bands at 1350, 1440, and 1505 cm^{-1} and a broader feature between 1110 and 1230 cm^{-1}. The computed spectrum of the free tetracation $\mathbf{1}^{4+}$ (blue trace in Figure 5) matches the experimental data reasonably well, and particularly the intense peak at 1630 cm^{-1} is nicely consistent with a computed feature at 1635 cm^{-1}. As far as band positions are concerned, the largest difference occurs for the computed band at 1120 cm^{-1}, whose correspondent in the experimental spectrum is some 30 cm^{-1} blue-shifted. Larger differences occur with respect to intensities, but these are anyhow to be considered more cautiously because of the multiphotonic excitation mechanism in IRMPD action spectroscopy.[14,36] The largest deviation concerns the band at 1630 cm^{-1} which has a larger relative abundance in experiment than predicted by theory. In this respect, we would like to draw attention to the stepwise nature of the fragmentation monitored in this particular case. Specif-

(32) Roithová, J.; Schröder, D.; Schwarz, H. *J. Phys. Chem. A* **2004**, *108*, 5060.
(33) Other small organic tetracations known so far are derived from polycyclic compounds such as ovalene or fullerenes (see ref 21a,d).
(34) Lammertsma, K.; Schleyer, P. R. v.; Schwarz, H. *Angew. Chem., Int. Ed. Engl.* **1989**, *28*, 1321.
(35) For previous examples of IRMPD spectra of mass-selected multiply charged ions, see: (a) Zhou, J.; Santambrogio, G.; Brümmer, M.; Moore, D. T.; Wöste, L.; Meijer, G.; Neumark, D.; Asmis, K. R. *J. Chem. Phys.* **2006**, *125*, 111102. (b) Fukui, K.; Takada, Y.; Sumiyoshi, T.; Imai, T.; Takahashi, K. *J. Phys. Chem. B* **2006**, *110*, 16111.
(36) (a) Riveros, J. M. In *Encyclopedia of Mass Spectrometry*; Armentrout, P. B., Ed.; Elsevier: Amsterdam, The Netherlands, 2003; Vol. 1, p 262. (b) Dopfer, O. *J. Phys. Org. Chem.* **2006**, *19*, 540.

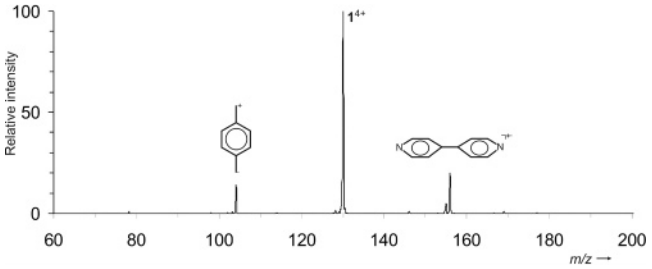

Figure 3. CID mass-spectrum of $\mathbf{1}^{4+}$ in the presence of xenon as a collision gas (collision energy 25 eV in the laboratory frame) leading to the monocations $C_8H_8^+$ ($m/z = 104$) and $C_{10}H_8N_2^+$ ($m/z = 156$). In addition, some fragments due to subsequent monocation dissociations are observed, e.g., $C_5H_4N^+$ ($m/z = 78$) and $C_{10}H_7N_2^+$ ($m/z = 155$). The initially formed dicationic fragment $C_{18}H_{16}N_2^{2+}$ cannot be seen, as it bears the same mass-to-charge ratio as the parent tetracation.

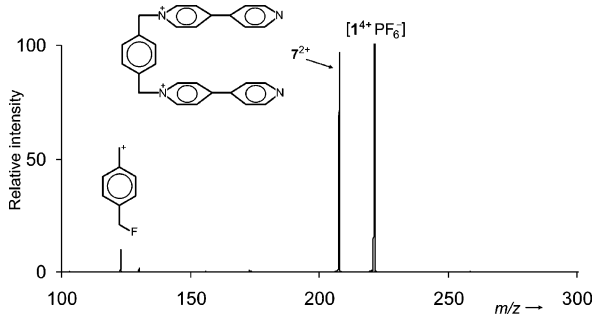

Figure 4. CID mass-spectrum of the trication $[\mathbf{1}^{4+}\cdot PF_6^-]$ in the presence of xenon as a collision gas (collision energy 25 eV in the laboratory frame) leading to the dication $C_{28}H_{24}N_4^{2+}$ ($m/z = 208$) and the monocation $C_8H_8F^+$ ($m/z = 123$) as the major products. Note that the parent trication is off-scale.

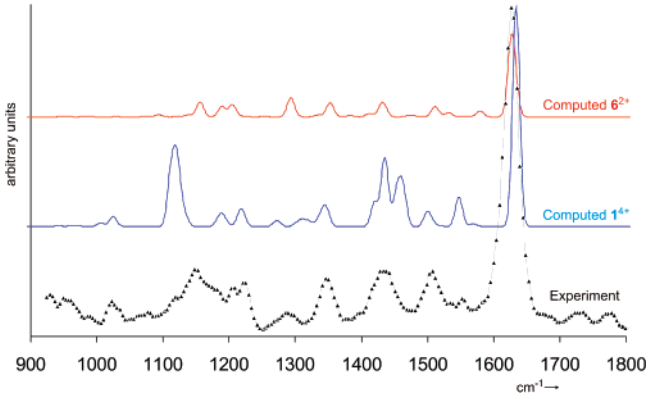

Figure 5. Experimental IRMPD spectrum of mass-selected $\mathbf{1}^{4+}$ between 900 and 1800 cm^{-1} (triangles) and computed IR spectrum (blue) of $\mathbf{1}^{4+}$ and of the dicationic fragment $C_{18}H_{16}N_2^{2+}$ (red) in the same spectral range. The experimental spectrum is an average of two independent acquisitions.

ically, in the present IRMPD experiments performed with an ion-trap mass spectrometer, ion dissociation is only monitored by means of the monocationic fragments (reaction 2), whereas the primary fragmentation of the tetracation according to reaction 1 remains invisible in the IT−MS. As a consequence, the IR bands of the dicationic intermediate $C_{18}H_{16}N_2^{2+}$ will also contribute to the experimental spectrum. In fact, the intermediate $C_{18}H_{16}N_2^{2+}$ dication $\mathbf{6}^{4+}$ also shows a pronounced adsorption at 1630 cm^{-1} (red trace in Figure 5), such that the propensity for ion dissociation to the finally measured monocation fragments is expected to be particularly large for this band. Note, however, that a precise deconvolution of the components is not trivial (see ref 14), and given the noise level of the experimental

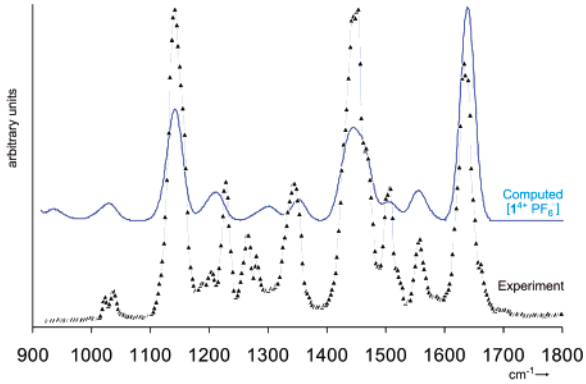

Figure 6. Experimental IRMPD spectrum of mass-selected $[\mathbf{1}^{4+}\cdot PF_6^-]$ between 900 and 1800 cm^{-1} (triangles) and computed IR spectrum (blue) in the same spectral range.

Chart 2. Computed Structures of the Tetracation $\mathbf{1}^{4+}$, the Corresponding Trication Bearing One PF_6^- Counterion, and the Doubly Charged Fragment $\mathbf{6}^{2+}$ (B3LYP/6-31G**)

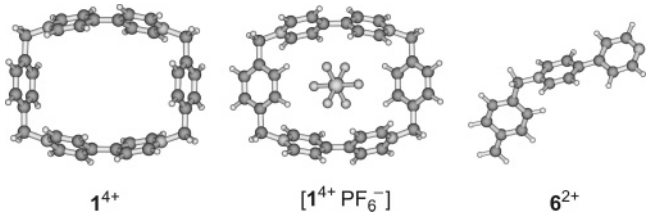

data we refrained from a more detailed analysis. Notwithstanding these minor discrepancies between experiment and theory, the IRMPD data lend further confidence that the intact tetracation $\mathbf{1}^{4+}$ is indeed monitored experimentally. We note however, that the IRMPD spectra do not permit a clear-cut distinction between $\mathbf{1}^{4+}$ and its dicationic fragment $\mathbf{6}^{2+}$ owing to the overall similarity of the computed IR spectra in the range investigated.

In addition, the adduct with one hexafluorophosphate anion has been investigated by means of IRMPD. Compared to the tetracation, the spectrum of $[\mathbf{1}^{4+}\cdot PF_6^-]$ is more structured (Figure 6), even though the major bands appear at similar positions, i.e., at about 1140, 1450, and 1630 cm^{-1}. Again, reasonable agreement exists between experiment and theory (blue trace in Figure 6) as far as the positions of the bands are concerned with the largest deviation for the bands between 1200 and 1300 cm^{-1}. As expected, larger differences occur between the computed and measured intensities, but the agreement between experiment and theory can be considered as being reasonable. Because the computed spectrum refers to the tetracation $\mathbf{1}^{4+}$ having a PF_6^- anion as a guest in the center of the macrocycle, we consequently conclude that the hexafluorophosphate is located in the cavity of $\mathbf{1}^{4+}$ rather than being loosely bound to the outer periphery of the multiply charged ion.

In the context of the computational work, we note further that the ab initio calculations predict an overall exothermicity of 2.9 eV for the charge separation of the tetracation $\mathbf{1}^{4+}$ into two equal dications according to reaction 1. As far as ion structures are concerned (Chart 2), the computations also reflect the anticipated repulsion of the positive charges in the free catenane in that the circumference (measured as the sum of the distances between the four nitrogen atoms) amount is slightly larger in free $\mathbf{1}^{4+}$ (27.66 Å) compared to $[\mathbf{1}^{4+}\cdot PF_6^-]$ (27.56 Å) with the bulky hexafluorophosphate as a guest in the cavity. We note for the sake of completeness that the dicationic

Scheme 2. Sketch of the Fragmentation of the Tetracation $\mathbf{2}^{4+}$ to the Dications $\mathbf{7}^{2+}$ ($m/z = 208$) and $\mathbf{8}^{2+}$ ($m/z = 140$) via Cleavage of the Two C−N Bonds in Close Proximity to the Triptycene Linker

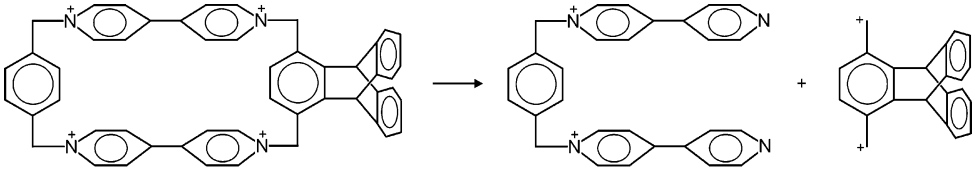

$\mathbf{2}^{4+}$ $\mathbf{7}^{2+}$ $\mathbf{8}^{2+}$

fragment $\mathbf{6}^{2+}$ bears an enlarged central CCN angle (at the benzylic methylene group), as expected from the Coulombic repulsion of the charge centers.

Yet another chemical evidence for the existence of intact $\mathbf{1}^{4+}$ in the gas phase is provided by the thermal reactivity of the mass-selected tetracation in that it does not react with either water or benzene, although these are otherwise good reaction partners for proton- and electron-transfer reactions, respectively.[10,37] With neutral methanol, however, a clean shift by $\Delta m = +8$ amu is observed, which can be assigned to the incorporation of methanol as a guest molecule in the cavity of the tetracation $\mathbf{1}^{4+}$. To the best of our knowledge, this is the first example of an ion/molecule reaction of a medium-sized tetracation in the gas phase with maintenance of the 4-fold charge. Conceptually, the observation of this particular reaction also offers prospects for studies toward molecular recognition, in that the uptake of guest molecules by the multiply charged host is likely to be crucially dependent on the chemical nature of the guest.

In addition to the parent compound $\mathbf{1}^{4+}$, two derivatives were examined, in which one or both 1,4-benzoquinodimethano linkers are replaced by a triptycene skeleton, that is, $\mathbf{2}^{4+}$ and $\mathbf{3}^{4+}$ (Chart 1). The comparison thus permits an investigation of how the size of the tetracation influences the dissociation behavior.

$$C_{50}H_{40}N_4^{4+}\ (\mathbf{2}^{4+}) \rightarrow C_{32}H_{24}N_2^{2+} + C_{18}H_{16}N_2^{2+} \quad (4)$$

$$\rightarrow C_{28}H_{24}N_4^{2+} + C_{22}H_{16}^{2+} \quad (5)$$

Compound $\mathbf{2}^{4+}$ bears a triptycene linker on one side of the macrocycle. Upon CID, the tetracation undergoes cleavage of two distant C−N bonds in analogy to reaction 1, but because of the reduced symmetry of this compound, two dicationic fragments of different mass-to-charge ratios are formed (reaction 4). Interestingly, a similarly abundant competing fragmentation is observed, which can be attributed to the occurrence of two C−N bond cleavages in an asymmetrical fashion to afford the dications $\mathbf{7}^{2+}$ and $\mathbf{8}^{2+}$, respectively (reaction 5, Scheme 2).

For the corresponding trication with one counterion, $[\mathbf{2}^{4+}\cdot PF_6^-]$, CID leads again to a formal substitution by a fluoride ion (reaction 6).

$$[\mathbf{2}^{4+}\cdot PF_6^-] \rightarrow C_{28}H_{24}N_4^{2+} + C_{22}H_{16}F^+ + PF_5 \quad (6)$$

$$\rightarrow C_{42}H_{32}N_4^{2+} + C_8H_8F^+ + PF_5 \quad (7)$$

Discrimination effects in ion detection are less severe in this case, in that the di- and monocationic fragments are detected in a ca. 3:1, compared to a difference of almost an order of magnitude for $[\mathbf{1}^{4+}\cdot PF_6^-]$ (Figure 4). This finding suggests that primarily the ion mass, rather than the mere charge, is the major factor in ion discrimination in the triple-quadrupole instrument used in these studies. Conceptually, the substitution by fluoride can occur in two fashions for the nonsymmetrical ion $\mathbf{2}^{4+}$, in that fluoride can either attack at the benzoquinodimethano or the triptycene linker. Nevertheless, reaction 6 is largely preferred over the competing process according to reaction 7 in that the corresponding dication fragment $C_{42}H_{32}N_4^{2+}$ is about 2 orders of magnitude less abundant than $C_{28}H_{24}N_4^{2+}$ and $C_8H_8F^+$ hardly is detected.

$$C_{64}H_{48}N_4^{4+}\ (\mathbf{3}^{4+}) \rightarrow 2C_{32}H_{24}N_2^{2+} \quad (8)$$

$$C_{32}H_{24}N_2^{2+} \rightarrow C_{11}H_{10}N_2^{+} + C_{21}H_{14}^{+} \quad (9)$$

$$[\mathbf{3}^{4+}\cdot PF_6^-] \rightarrow C_{42}H_{32}N_4^{2+} + C_{22}H_{16}F^+ + PF_5 \quad (10)$$

For the compound with two triptycene linkers, the tetracation $\mathbf{3}^{4+}$, the results obtained are again very close to that of the parent compound, in that CID leads to a symmetrical cleavage into two identical dications (reaction 8), which again can only be monitored by mass selection of the natural $^{13}C_1$-isotope of $\mathbf{3}^{4+}$. Subsequent charge separations of the dicationic fragments then follow a slightly different route compared to the parent compound $\mathbf{1}^{4+}$, in that cleavage of the C−C bond takes place at the triptycene to (formally) afford the methylene ylide ion of bipyridyl, $CH_2-C_5H_4N-C_5H_4N^{+\bullet}$, and a $C_{21}H_{14}^{+}$ fragment (reaction 9), rather than C−N bond cleavage as observed for the dication formed from $\mathbf{1}^{4+}$ (see Scheme 1). For the trication $[\mathbf{3}^{4+}\cdot PF_6^-]$, fluoride attack at the benzylic position is again observed (reaction 10).

In summarizing the findings reported so far, we can draw the following conclusions. At first, the gaseous tetracations $\mathbf{1}^{4+}$–$\mathbf{3}^{4+}$ are kinetically stable entities in the gas phase in that separation to fragments of reduced charge only takes place upon CID. For the symmetrical compounds, the preferred dissociation pathways involve a symmetrical cleavage of two remote C−N bonds (path A in Scheme 3), whereas the nonsymmetrical compound $\mathbf{2}^{4+}$ also undergoes a cleavage of two proximate C−N bonds (path B in Scheme 3). While the precise energetics of channels A and B are unknown, the different branching ratios can be rationalized by a simple picture considering the stabilization of the 2-fold charges in the product dications. Path A leads to two identical dications, in which the positive charges in the dication products are, however, located relatively close to each other and the size of the molecules allows for an only limited

(37) Roithová, J.; Herman, Z.; Schröder, D.; Schwarz, H. *Chem.—Eur. J.* **2006**, *12*, 2465.

Scheme 3. Pathways for the Cleavage of the Tetracations $\mathbf{1}^{4+}$–$\mathbf{3}^{4+}$ upon CID

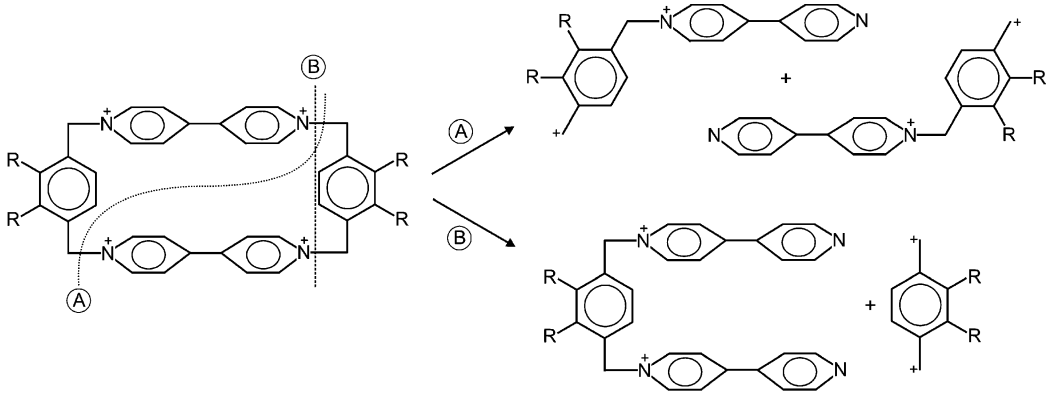

delocalization. In contrast, path B leads to a bis(bipyridylium) substituted xylene with an extended π-skeleton for charge delocalization. The price to pay though is the concomitant formation of a relatively small benzoquinodimethane dication. For $\mathbf{1}^{4+}$ (R = H), the large charge density in the small $C_8H_8^{2+}$ fragment which would be formed via path B suppresses this pathway, and only the symmetrical cleavage is observed. For the monotriptycene derivative $\mathbf{2}^{4+}$, both pathways become of comparable energy demand, because the substitution favors the formation of the benzoquinodimethane dication. In the case of $\mathbf{3}^{4+}$, however, the stabilizing effect of substitution is now also exerted in path A, and hence this route is preferred again.

In addition to the free tetrapyridinium cations, also their catenanes with the bis-*p*-phenylene-34-crown-10 (**4**) were investigated. In the case of **cat-1**$^{4+}$, ESI of a methanolic solution of the hexafluorophosphate yields an intense signal owing to the free tetracation **cat-1**$^{4+}$ with the expected isotope pattern and peak distances of 0.25 mass units. CID of the mass-selected catenane **cat-1**$^{4+}$ affords three ionic products: the bis(bipyridylium) substituted xylene fragment $C_{28}H_{24}N_4^{2+}$ ($\mathbf{7}^{2+}$), a benzochinodimethane monocation, and the ionized crown ether (Figure 7).

The product pattern implies dissociation of **cat-1**$^{4+}$ according to reaction 11; note that discrimination effects again favor detection of the dicationic product ion.

$$C_{64}H_{72}N_4^{4+}\ (\mathbf{cat\text{-}1}^{4+}) \rightarrow C_{28}H_{24}N_4^{2+} + C_8H_8^{+} + \mathbf{4}^{+} \quad (11)$$

$$\rightarrow 2\ C_{18}H_{16}N_2^{2+} + \mathbf{4} \quad (12)$$

Thus, the presence of the crown ether enables the nonsymmetrical cleavage (path **B** in Scheme 3) to occur, because intermediate electron transfer avoids the formation of the energetically unfavorable $C_8H_8^{2+}$ dication. Interestingly, the symmetrical cleavage to afford two $C_{18}H_{16}N_2^{2+}$ dications (reaction 12) is hardly observed upon CID of **cat-1**$^{4+}$, whereas this pathway gives rise to the base peak upon fragmentation of free $\mathbf{1}^{4+}$.

For the substituted compounds **cat-2**$^{4+}$ and **cat-3**$^{4+}$, the situation is more problematic, because these catenanes do not dissolve in pure methanol or methanol/water mixtures. While the compounds can be dissolved in mixtures containing more dipolar solvents, such as acetone or acetonitrile, ESI of these solutions primarily leads to complexes of the tetracations with the particular solvent molecules, that is, [**cat-2**$^{4+}\cdot L_n$] and [**cat-3**$^{4+}\cdot L_n$] with L = acetone or acetonitrile and n = 1–4. At harsher ionization conditions, which generally favor desolvation of gaseous ions produced via ESI, also a significant amount of dissociation of the tetracations takes place, such that the yields of the free tetracations remain poor. MS/MS experiments with bare **cat-2**$^{4+}$ and **cat-3**$^{4+}$ were thus only possible at a reduced mass resolutions without selection of a particular ^{13}C isotope. Likewise, the resolution of the analyzing quadrupole had to be lowered because of the low ion abundances, which renders the assignment of the product ions somewhat less certain. With the reservation that a precise assignment of the fragments' charge states cannot be made on grounds of intensities, the major dissociation reactions follow reaction 11, that is, cleavage of two neighbored C–N bonds following pathway B (Scheme 3) leading to a dication containing all four pyridine rings, a singly ionized linker, and the ionized guest molecule. In the case of the unsymmetrical catenane **cat-2**$^{4+}$, cleavage according to path B in Scheme 3 again shows a strong preference for the formation of the triptycene-substituted dication fragment. Hence, the fragmentations of the catenane tetracations by and large follow those of the corresponding free tetracations with the difference being that the incorporated crown ether delivers one electron upon fragmentation as shown for **cat-1**$^{4+}$ in reaction 11.

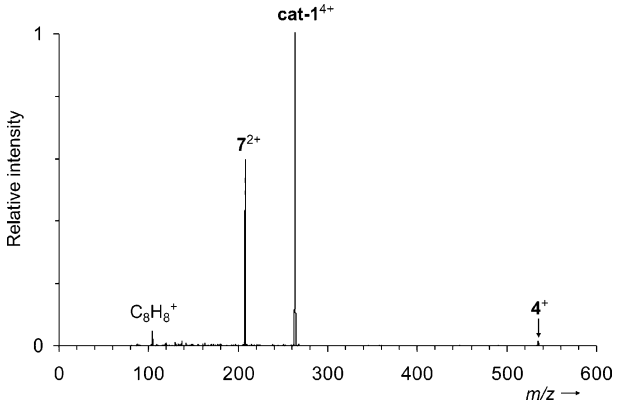

Figure 7. CID mass-spectrum of the catenane tetracation **cat-1**$^{4+}$ (collision gas, xenon; collision energy, 25 eV in the laboratory frame). Note that the parent tetracation is off-scale.

4. Conclusions

By means of electrospray ionization, Stoddart's cyclobis(paraquat-*p*-phenylene) can be transferred into the gas phase. Free $\mathbf{1}^{4+}$ and its triptycene derivatives $\mathbf{2}^{4+}$ and $\mathbf{3}^{4+}$ are among the very few examples of long-lived molecular tetracations of medium size known so far. Moreover, the present results demonstrate that these tetracations can undergo bimolecular reactions in the gas phase without the occurrence of concomitant electron transfer. Dissociation of the tetracations occurs via C−N bond cleavage of the pyridinium ions to afford pairs of dications which subsequently undergo charge separation to monocationic products. Chemical as well as spectroscopic evidence demonstrates that isolated $\mathbf{1}^{4+}$ can exist as a long-lived tetracation in the gas phase. In addition to the free tetracations $\mathbf{1}^{4+}$−$\mathbf{3}^{4+}$, their adducts with one hexafluorophosphate counterion as well as the corresponding catenanes with a benzo-crown ether are investigated. Dissociation of the hexafluorophosphate adducts involves C−N bond cleavage of the pyridinium ions concomitant with C−F bond formation, whereas the catenane tetracations show electron transfer from the guest molecules to the tetracationic host. In all cases studied here, a key motif is the enormous stabilization of the high charge states in these multiply charged ions by the cyclic pyridinium backbone. Once the macrocycle begins to fragment, however, electron-transfer processes can take place, which leads to bond cleavage and also electron transfer in the case of the catenanes. In future work, we will investigate the properties of these free tetracations in bimolecular reactions, possibly also including processes in which molecular recognition can be mimicked.

Acknowledgment. Dedicated to Sir J. F. Stoddart on the occasion of his 65th birthday. The authors thank O. Miljanic and J. F. Stoddart for the helpful comments. Further, we appreciate the assistance of the entire staff of CLIO during the IRMPD measurements, which were also supported by the European Commission. T.B. is grateful for support of his work by the EPITOPES project, funded by the European Commission through the NEST program. Further, we thank M. Buděšínský (Prague) for ^{1}H and ^{13}C NMR measurements and D. Kuck (Bielefeld) for helpful comments about $C_8H_8^{+/2+}$ cations.

Supporting Information Available: Complete ref. 9, details of the synthesis of compounds **2** and **3**, and the Cartesian coordinates of the computed structures. This material is available free of charge via the Internet at http://pubs.acs.org.

JA071058H